

## Interfacial Layer Formation during Crystallization of Sol-Gel Derived SrBi<sub>2</sub>Ta<sub>2</sub>O<sub>9</sub> Thin Films on Silicon

A. Kohno and K. Matuo\*

Department of Applied Physics, Fukuoka University, 8-19-1 Nanakuma, Jonan-ku, Fukuoka 814-0180, Japan.  
Fax: +81-92-871-6631, e-mail: kohno@fukuoka-u.ac.jp

Ferroelectric SrBi<sub>2</sub>Ta<sub>2</sub>O<sub>9</sub> (SBT) thin films have been formed on silicon substrates at a crystallization temperature as low as 750 °C. The crystallization atmosphere (O<sub>2</sub>, N<sub>2</sub>, H<sub>2</sub>O-vapor/N<sub>2</sub>) influenced the electrical characteristics of the Au/SBT/p-Si structures. The capacitance-voltage characteristics of the devices suggested that the defects in the interface region were smallest as the SBT film was crystallized in the H<sub>2</sub>O-vapor/N<sub>2</sub> atmosphere. The effect of the crystallization atmosphere on the SBT film and interface structures were quantitatively investigated by using X-ray reflectivity (XRR) method. It was confirmed that an interfacial layer was formed between the SBT film and the silicon substrate in any case. The interfacial layer was thickest in the case of H<sub>2</sub>O-vapor/N<sub>2</sub> atmosphere. However, the density of the interfacial layer was independent of the crystallization atmosphere. Furthermore, the crystallization duration dependence showed that the thickness of the interfacial layer increased with crystallization duration but the density remained a value ~2.5 g/cm<sup>3</sup>. The interfacial layer formation was mainly caused by oxidation of silicon.

Key words: ferroelectric thin film, SrBi<sub>2</sub>Ta<sub>2</sub>O<sub>9</sub> (SBT), interfacial layer, X-ray reflectivity, crystallization

### 1. INTRODUCTION

Nonvolatile ferroelectric memories using field-effect transistors (FETs) with a ferroelectric thin film as a gate insulator have been attractive because of some advantages of nondestructive readout operation and device-scaling capabilities [1]. In recent years metal-ferroelectric-insulator-semiconductor (MFIS) FETs have been researched because the interface states crucially affect the FET performance and the formation of an interfacial oxide layer between the ferroelectrics and the Si substrate may be unavoidable [1]. Nevertheless, the direct formation of ferroelectric films on Si substrates is attractive because of the possibility of controlling the in-plane orientation [2]. At all events, it is important for the development of the MF(I)SFET-type memories to research the interfacial layer formation and to develop the improvement processes. One of the possible processes for the improvement of the film and interface qualities has been developed [3]. By the annealing the SiO<sub>2</sub>/poly-Si samples in the atmosphere including H<sub>2</sub>O vapor the defects in the film and at the interface were well reduced. It is worth while investigating the effect of this annealing on the ferroelectric/Si and/or ferroelectric/insulator/Si structures.

Strontium bismuth tantalate (SrBi<sub>2</sub>Ta<sub>2</sub>O<sub>9</sub>; SBT) thin film has been recognized as a potential candidate for nonvolatile memory applications because of its excellent fatigue-free and lead-free natures [4]. The formation processes of SBT thin films have been widely researched [5-8] and the crystallization and grain growth of the SBT film have been investigated [5, 9]. The

electrical characteristics of the MFS and MFIS structures with SBT films have been researched [10-19] and the long data retention of the MFIS-FETs has been reported [17-19]. However, the control of the interface states and the device performance is so difficult and further research of the interface is necessary.

In this study, we investigated the effects of the atmosphere during the crystallization of the SBT films on the electrical and structural characteristics of SBT/Si structures. X-ray reflectivity (XRR) method was employed to analyze the structures of the SBT film/Si samples without destruction of the sample [20-22].

### 2. EXPERIMENTAL

P-type Si(100) wafers were cleaned by chemical solutions to remove metal contaminations. After the wafers were treated with diluted HF solution to obtain hydrogen-terminated surfaces, a sol-gel precursor solution produced by Kanto Chemical Co., Inc., was spin-coated on the Si substrates. The coated wafers were dried on a hot plate at 150 °C for 30 min. Subsequently, the samples were crystallized at temperatures of 750-770 °C in a furnace. During crystallization N<sub>2</sub>, O<sub>2</sub> gas or N<sub>2</sub> gas including H<sub>2</sub>O vapor (H<sub>2</sub>O-vapor/N<sub>2</sub>) was introduced to the furnace at a flow rate of 500ml/min. To generate the H<sub>2</sub>O-vapor/N<sub>2</sub>, N<sub>2</sub> carrier gas was bubbled in the ultra-pure water warmed at 95 °C.

The thickness, density and roughness of each layer were evaluated by XRR analysis, and also crystallization of the film was observed by X-ray diffraction (XRD). X-ray reflection and diffraction measurements were carried out using the diffractometer with an Eulerian cradle and a graded multilayer mirror. The incident

\*Present affiliation: Memory Division, TOSHIBA Corporation Semiconductor Company

X-ray ( $\text{CuK}\alpha$ ) radiation was converted into a quasi-monochromatic and parallel beam by the mirror, and the diffracted or reflected X-ray by the sample was detected through the solar slit and the graphite monochromator. In the case of XRD measurements, the glancing angle of the incident beam from the surface was fixed and the detector was scanned ( $2\theta$  scan). For measurement of the electrical characteristics the gold dots were deposited on the film as the gate electrodes. All measurements were carried out at room temperature.

### 3. RESULTS AND DISCUSSION

#### 3.1 Ferroelectric film formation and electrical properties

The XRD profiles as a function of crystallization duration are shown in Fig. 1 in the case of the  $\text{H}_2\text{O}$ -vapor/ $\text{N}_2$  annealing at  $770^\circ\text{C}$ . The intensity of the peaks labeled "S" for the orthorhombic phase (ferroelectric) with the space group  $A2_1am$  (Bi-layered Aurivillius phase) increased and that labeled "F" for the fluorite-type (space group:  $Fm3m$ ) decreased with the duration [5, 23]. This phase transformation from the fluorite to the orthorhombic phase was the same as that reported elsewhere [24] and almost independent of the crystallization atmosphere. Since the fluorite-type phase is not ferroelectric, the film must be annealed enough to form the single Aurivillius phase. On the other hand, the crystallization duration should be shortened because the thicker interfacial oxide grows with the longer duration and the interfacial layer with a lower dielectric constant is undesirable for the device characteristics, as described later.

A typical capacitance-voltage characteristic for the Au/SBT/p-Si structure with the SBT film crystallized at  $770^\circ\text{C}$  in  $\text{H}_2\text{O}$ -vapor/ $\text{N}_2$  is shown in Fig. 2. The crystallization duration was set to 90 min for formation of the single Aurivillius-phase SBT (see Fig. 1). Measurement frequency was 1MHz. Clockwise

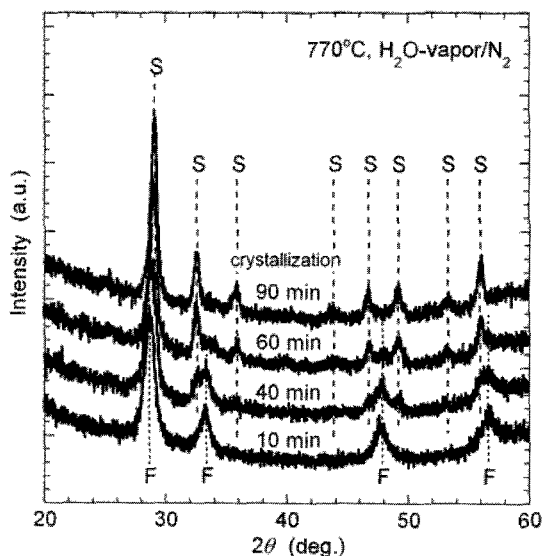


Fig. 1 X-ray diffraction profiles from the SBT film as a function of crystallization duration in the  $\text{H}_2\text{O}$ -vapor/ $\text{N}_2$  at  $770^\circ\text{C}$ . The denotation "S" is for the diffraction peak of the orthorhombic phase and "F" is for that of fluorite-type phase.

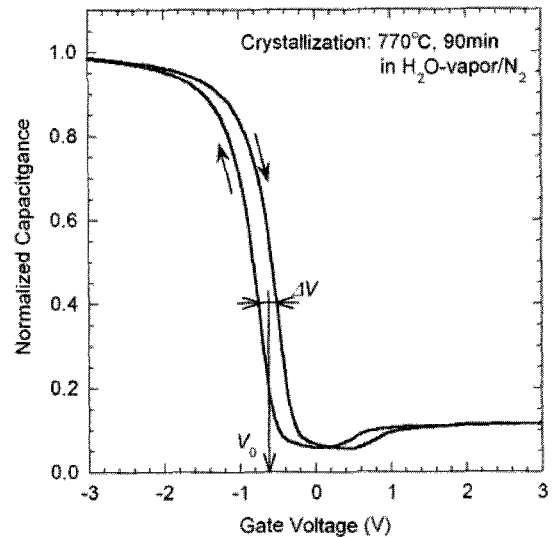


Fig. 2 Typical capacitance-voltage characteristics of Au/SBT/p-Si structure. The SBT film was crystallized in  $\text{H}_2\text{O}$ -vapor/ $\text{N}_2$  at  $770^\circ\text{C}$ . The gate bias was swept between  $+5$  and  $-5$  V.

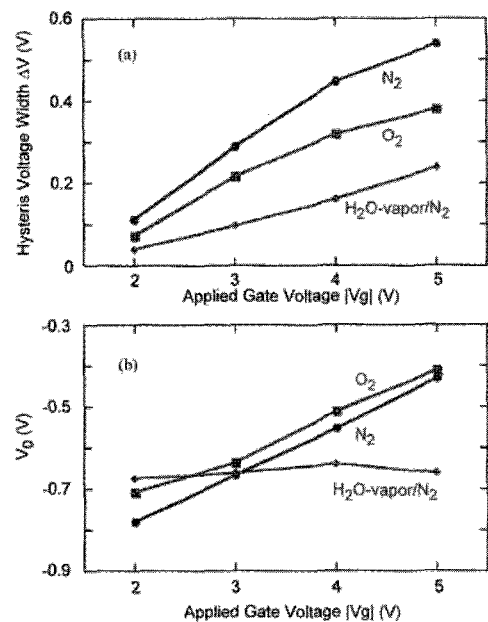


Fig. 3 Applied gate voltage dependence of (a) the hysteresis voltage width and (b) the middle voltage of the C-V hysteresis of the Au/SBT/p-Si capacitor.

hysteresis was due to ferroelectric nature of the SBT film. The hysteresis voltage width  $\Delta V$  and the middle voltage of the hysteresis  $V_0$  were evaluated as a function of the applied gate voltage. The  $\Delta V$  depended on the applied gate voltage in any case, as shown in Fig. 3(a). The  $\Delta V$  values for the SBT crystallized in  $\text{H}_2\text{O}$ -vapor/ $\text{N}_2$  were smallest. This small  $\Delta V$  was probably caused by the interfacial layer with low dielectric constant, as discussed later. As shown in Fig. 3(b), the  $V_0$  value in  $\text{H}_2\text{O}$ -vapor/ $\text{N}_2$  case was independent of the applied gate voltage, whereas those in  $\text{O}_2$  and  $\text{N}_2$  cases increased

with increasing the applied voltage. The positive shift of  $V_0$  corresponds to that of the flat-band voltage of a metal-insulator-semiconductor (MIS) capacitor. This positive shift was probably caused by the electron injection to the trap states at and/or near the SBT/Si interface. Although the Au/SBT interface also affects the device characteristics, for the voltage shift the electron traps at the SBT/Si interface is more effective than that at the Au/SBT interface and the crystallization atmosphere affects almost the formation of the SBT/Si interface because the Au gate electrodes were fabricated after crystallization. Therefore, the difference of the  $V_0$  shift is attributed to the SBT/Si interface states. Since the electron injection was enhanced with increasing the gate bias, the  $V_0$  value increased. The results suggest that the crystallization in  $H_2O$ -vapor/ $N_2$  is effective to obtain high quality interface and film from the viewpoint of the electrical characteristics.

### 3.2 Film and interfacial layer structures

The structure of SBT/Si samples was analyzed by XRR method. The XRR spectra from the SBT/Si samples, the SBT films of which are crystallized at  $750^\circ C$  for 60 min, are shown in Fig. 4. The simulation fitting using the three layer model shown in the inset of Fig. 4 was carried out. The best fit curves are also shown in Fig. 4. In the case of  $H_2O$ -vapor/ $N_2$  the oscillation amplitude was rapidly damped. This was attributed to the rougher surface and interface, indicating that the grain growth was enhanced in the  $H_2O$ -vapor/ $N_2$  case in consistency with AFM observation.

The simulated results are summarized in Fig. 5. The density of the SBT layer was lower than that of the single crystal reported by Rae *et al.* [23], indicating that the film contains many defects and low-density grain-boundary regions [24]. The interfacial layer was thickest in the  $H_2O$ -vapor/ $N_2$  case, while the density was almost independent of the crystallization atmosphere.

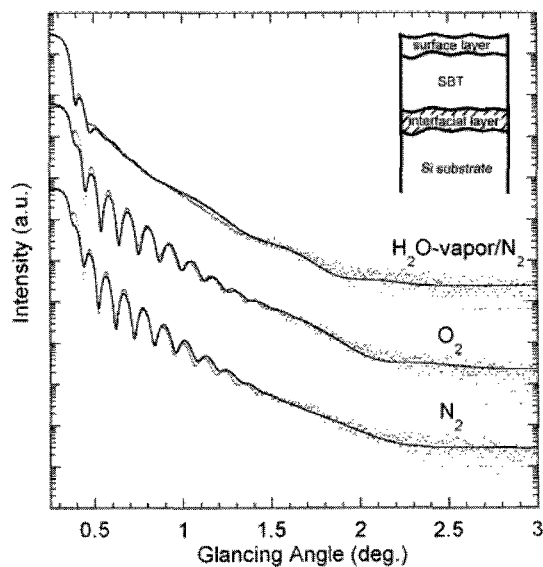


Fig. 4 Change in X-ray reflectivity spectrum for the SBT/Si structures by the crystallization atmosphere. The dots are for the measured data and the curves are for the best fit results.

These results suggest that the interfacial layer was mainly caused by oxidation of silicon. Furthermore, the reason for smaller hysteresis width as shown in Fig. 3 is because the thicker interfacial layer, the dielectric constant of which is probably as low as  $SiO_2$ , reduces the effective voltage across the SBT layer. This undesirable effect is a trade-off for a reduction of the electron traps at the interface.

The XRR spectra as function of crystallization duration are shown in Fig. 6. The simulated curves using the same model as that in Fig. 4 are also shown. The annealing time dependence of the thickness and the

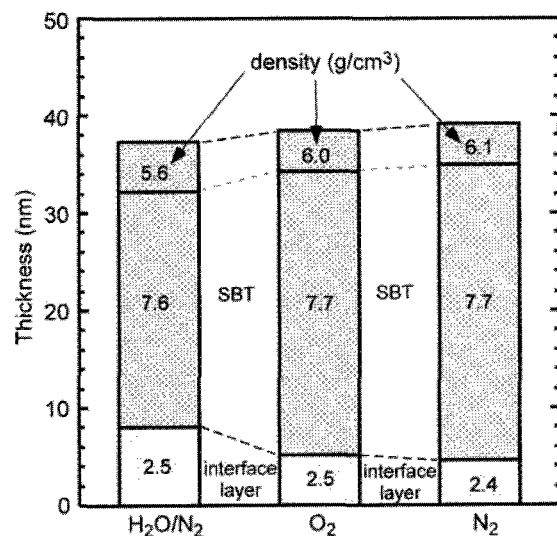


Fig. 5 Layer thickness and density evaluated by X-ray reflectivity analysis.

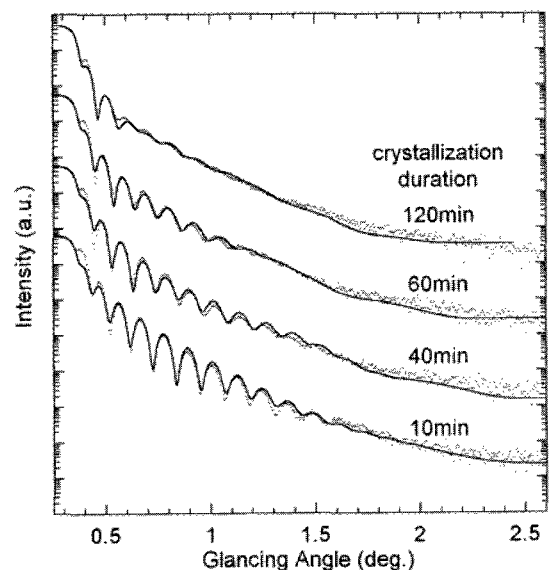


Fig. 6 X-ray reflectivity spectra for the SBT/Si structure as a function of crystallization duration. The SBT thin film was crystallized in  $H_2O$ -vapor/ $N_2$  at  $750^\circ C$ . The dots are for the measured data and the curves are for the best fit results. The fitting model was same as that in Fig. 4.

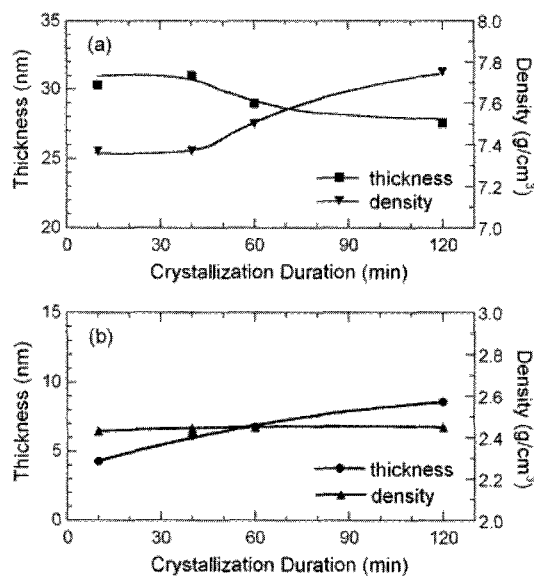


Fig. 7 The crystallization duration dependence of the thickness and density for (a) the SBT layer and (b) the interfacial layer.

density for the SBT layer and for the interfacial layer are shown in Fig. 7(a) and 7(b), respectively. The SBT layer thickness was reduced and the density increased with crystallization time as shown in Fig. 7(a). This fact means the densification of the SBT layer. On the other hand, the thickness of the interfacial layer increased but the density was kept constant. This is consistent with the previous result, suggesting that the interfacial layer was formed by oxidation of silicon.

#### 4. CONCLUSIONS

The effect of the crystallization atmosphere ( $\text{O}_2$ ,  $\text{N}_2$ ,  $\text{H}_2\text{O}$ -vapor/ $\text{N}_2$ ) on the electrical and structural characteristics of the SBT/Si structures were investigated. The capacitance-voltage characteristics of the Au/SBT/p-Si structures depended on the atmosphere during crystallization. The hysteresis due to ferroelectric nature of SBT film was observed in the C-V characteristics. The characteristics suggested that the defects near the interface were smallest in the case of  $\text{H}_2\text{O}$ -vapor/ $\text{N}_2$ . However, the hysteresis voltage width of the C-V curves was reduced as the film was crystallized in the  $\text{H}_2\text{O}$ -vapor/ $\text{N}_2$  atmosphere. This smaller hysteresis was because the effective voltage across the SBT layer was reduced by the thicker interfacial layer. The XRR analysis showed that the interfacial layer was thickest in the case of  $\text{H}_2\text{O}$ -vapor/ $\text{N}_2$  atmosphere. On the other hand, the density of the interfacial layer was independent of the crystallization atmosphere. With the crystallization duration the thickness of the interfacial layer increased but the density remained a value  $\sim 2.5 \text{ g/cm}^3$ . The dependences on the crystallization atmosphere and duration suggested that the interfacial layer formation was mainly caused by oxidation of silicon.

#### Acknowledgements

This work was supported in part by funds (No. 055004)

from the Central Research Institute of Fukuoka University.

#### References

- [1] H. Ishiwara, "Ferroelectric Film Devices" (Handbook of Thin Film Devices, vol. 5), ed. by D. J. Taylor, Academic Press, San Diego (2000) Chap. 3, pp. 79-88.
- [2] A. Kohno, F. Ishitsu, K. Matuo and H. Tomari, *Mater. Res. Soc. Symp. Proc.*, **784**, 497-502 (2004).
- [3] N. Sano, M. Sekiya, M. Hara, A. Kohno and T. Sameshima, *Appl. Phys. Lett.*, **66**, 2107-2109 (1995).
- [4] C. A. Paz de Araujo, J. D. Cuchiaro, L. D. McMillan, M. C. Scott and J. F. Scott, *Nature*, **374**, 627-629 (1995).
- [5] T. Ami, K. Hironaka, C. Isobe, N. Nagel, M. Sugiyama, Y. Ikeda, K. Watanabe, A. Machida, K. Miura and M. Tanaka, *Mater. Res. Soc. Symp. Proc.*, **415**, 195-200 (1996).
- [6] T. Hayashi, T. Hara and H. Takahashi, *Jpn. J. Appl. Phys.*, **36**, 5900-5903 (1997).
- [7] J. H. Cho, S. H. Bang, J. Y. Son and Q. X. Jia, *Appl. Phys. Lett.*, **72**, 665-667 (1998).
- [8] N. Nukaga, K. Ishikawa and H. Funakubo, *Jpn. J. Appl. Phys.*, **38**, 5428-5431 (1999).
- [9] J. H. Choi, J. Y. Lee and Y. T. Kim, *Appl. Phys. Lett.*, **74**, 2933-2935 (1999).
- [10] E. Tokumitsu, G. Fujii and H. Ishiwara, *Mater. Res. Soc. Symp. Proc.*, **493**, 495-464 (1998).
- [11] T. Hirai, Y. Fujisaka, K. Nagashima, H. Koike and Y. Tarui, *Jpn. J. Appl. Phys.*, **36**, 5908-5911 (1997).
- [12] K. Sakamaki, T. Hirai, T. Uesugi, H. Kishi and Y. Tarui, *Jpn. J. Appl. Phys.*, **38**, L451-L453 (1999).
- [13] M. Noda, H. Sugiyama and M. Okuyama, *Jpn. J. Appl. Phys.*, **38**, 5432-5436 (1999).
- [14] H. Sugiyama, T. Nakaiso, Y. Adachi, M. Noda and M. Okuyama, *Jpn. J. Appl. Phys.*, **39**, 2131-2135 (2000).
- [15] B-E. Park and H. Ishiwara, *Appl. Phys. Lett.*, **79**, 806-808 (2001).
- [16] M. Noda, K. Kodama, I. Ikeuchi, M. Takahashi and M. Okuyama, *Jpn. J. Appl. Phys.*, **42**, 2055-2058 (2003).
- [17] S. Sakai, R. Ilangoan and M. Takahashi, *Jpn. J. Appl. Phys.*, **43**, 7876-7878 (2004).
- [18] K. Aizawa, B-E. Park, Y. Kawashima, K. Takahashi and H. Ishiwara, *Appl. Phys. Lett.*, **85**, 3199-3201 (2004).
- [19] M. Takahashi and S. Sakai, *Jpn. J. Appl. Phys.*, **44**, L800-L802 (2005).
- [20] E. Chason, "In Situ Real-Time Characterization of Thin Films", eds. by O. Auciello and A. R. Krauss, John Wiley & Sons, Canada, (2001) Chap. 6, p. 167.
- [21] V. Holy, U. Pietsch, T. Baumbach, "High-Resolution X-ray Scattering from Thin Films and Multilayers", Springer-Verlag, Berlin, (2001) Springer Tracts in Modern Physics Vol. 149, Chap.10, p. 191.
- [22] A. Kohno, H. Sakamoto, F. Ishitsu and K. Matuo, *Trans. Mater. Res. Soc. Jpn.*, **28**, 1203-1206 (2003).
- [23] A. D. Rae, J. G. Thompson and R. L. Withers, *Acta Cryst. B*, **48**, 418-428 (1992).
- [24] A. Kohno, H. Sakamoto, K. Matuo, *Jpn. J. Appl. Phys.*, **44**, 1928-1931 (2005).

(Received December 9, 2006; Accepted January 31, 2007)